Substrate Specificity and Oligomerization of Human GMP Synthetase

Martin Welin [1], Lari Lehtiö [1], Andreas Johansson [1], Susanne Flodin [1], Tomas Nyman [1], Lionel Trésaugues [1], Martin Hammarström [1], Susanne Gräslund [1] and Pär Nordlund [1,2]

*1 - **Structural Genomics Consortium,** Department of Medical Biochemistry and Biophysics, Karolinska Institutet, S-17177 Stockholm, Sweden*
*2 - **Centre for Biomedical Structural Biology,** School of Biological Sciences, Nanyang Technological University, 637551, Singapore*

***Correspondence to Pär Nordlund:** Structural Genomics Consortium, Department of Medical Biochemistry and Biophysics, Karolinska Institutet, S-17177 Stockholm, Sweden. Par.nordlund@ki.se*
http://dx.doi.org/10.1016/j.jmb.2013.06.032
Edited by J. Bowie

Abstract

Guanine monophosphate (GMP) synthetase is a bifunctional two-domain enzyme. The N-terminal glutaminase domain generates ammonia from glutamine and the C-terminal synthetase domain aminates xanthine monophosphate (XMP) to form GMP. Mammalian GMP synthetases (GMPSs) contain a 130-residue-long insert in the synthetase domain in comparison to bacterial proteins. We report here the structure of a eukaryotic GMPS. Substrate XMP was bound in the crystal structure of the human GMPS enzyme. XMP is bound to the synthetase domain and covered by a LID motif. The enzyme forms a dimer in the crystal structure with subunit orientations entirely different from the bacterial counterparts. The inserted sub-domain is shown to be involved in substrate binding and dimerization. Furthermore, the structural basis for XMP recognition is revealed as well as a potential allosteric site. Enzymes in the nucleotide metabolism typically display an increased activity in proliferating cells due to the increased need for nucleotides. Many drugs used as immunosuppressants and for treatment of cancer and viral diseases are indeed nucleobase- and nucleoside-based compounds, which are acting on or are activated by enzymes in this pathway. The information obtained from the crystal structure of human GMPS might therefore aid in understanding interactions of nucleoside-based drugs with GMPS and in structure-based design of GMPS-specific inhibitors.
© 2013 The Authors. Published by Elsevier Ltd. Open access under CC BY-NC-ND license.

Introduction

De novo synthesis of guanine nucleotides is essential for DNA and RNA synthesis. It also provides GTP, which is a key regulator and energy source in many cellular processes. Furthermore, it is involved in a number of cellular processes required for cell division. The final step in the *de novo* synthesis of guanine monophosphate (GMP) is catalyzed by GMP synthetase (GMPS; E.C. 6.3.5.2). GMPS belongs to the class 1 glutamine-dependent amidotranferases possessing a conserved catalytic triad consisting of a Cys, His, and Glu residue [1]. It catalyzes the conversion of xanthine monophosphate (XMP) to GMP in the presence of glutamine and ATP through an adenyl-XMP intermediate [2,3]. It is a bifunctional enzyme with two domains; the N-terminal glutaminase (GATase) domain generates ammonia from glutamine further used by the C-terminal synthetase domain to aminate XMP to yield GMP [4].

Several enzymes in the mammalian nucleotide metabolism display an increased activity in rapidly dividing cells due to an increased demand for nucleotides, thus making these enzymes targets for anti-cancer therapy [5]. Human GMPS (hGMPS) is also identified as a potential target for anti-cancer therapy [6–8]. Several glutamine analogs, like acivicin and 6-diazo-5-oxo-L-norleucine (DON) that bind covalently to the GATase site, have been observed to inhibit GMPS [9,10]. The preceding step in the *de novo* pathway making XMP from IMP is performed by IMP dehydrogenase and inhibitors of

this enzyme are now used for immunosuppressive and anti-viral chemotherapy [11]. There appears to be also additional roles for hGMPS in the cell. *Drosophila* GMPS is apparently involved in chromatin regulation [12] and axon guidance [13] and recently it was shown that hGMPS can allosterically enhance the activation of the ubiquitin-specific protease USP7/HAUSP [14].

Several GMPSs have been biochemically characterized, among these are hGMPS, as well as GMPS from *Escherichia coli* (*Ec*GMPS), *Pyrococcus horikoshii* OT3 GMPS (*Ph*GMPS), and *Plasmodium falciparum* GMPS [15–21]. Previously, a monomeric enzyme of hGMPS has been observed in solution [18,21]. The activity of hGMPS displays positive cooperativity for the substrate XMP, indicating allosteric regulation [18,21]. Structural information of GMPSs is available for several bacterial and archaeal enzymes. Structures of *Ec*GMPS in complex with AMP and pyrophosphate, *Thermus thermophilus* GMPS in complex with XMP [*Tt*GMPS; Protein Data Bank (PDB) ID: 2YWC], and the apo form of *Ph*GMPS have been determined and show similar overall folds and dimeric structures [1,20]. *Ec*GMPS was the first GMPS structure to be determined and revealed a distance between the two active sites of ca 30 Å [1]. During the reaction, the ammonia needs to be relocated from the GATase domain to the synthetase domain either by channeling or by domain rearrangement [1,4,22].

Here, we present the first structure of a eukaryotic GMPS, hGMPS, in complex with XMP. Interestingly, the structure reveals an additional sub-domain involved in substrate binding and dimerization. Furthermore, the structure defines the substrate specificity determinants for XMP. The fact that the hGMPS differs from its bacterial and archaeal counterpart by having an additional dimerization sub-domain interacting with the active site could be exploited in the development of potential anti-bacterial or anti-parasitic drugs.

Results

Overall structure of hGMPS

The structure of the hGMPS in complex with its substrate XMP was determined at 2.5 Å resolution. A monomer encompassing residues 20–693 of GMPS is composed of two catalytic domains, an N-terminal GATase domain (20–210) and a C-terminal synthetase domain (residues 220–693). The asymmetric unit contains a dimer. Residues 25–693 and 23–693 have been modeled for subunits A and B, respectively (Fig. 1a), with the exception of some flexible regions with no electron density in chain A (35–36, 79–85, 121–127, 312–321) and in chain B (123–125, 312–321). Although GMPS was co-crystallized with XMP, AMPPNP, and magnesium, only XMP is visible in the electron density map (Fig. 1b). Three sulfate ions are bound to each subunit (S1, S2, and S3). The synthetase domain can be divided into three separate sub-domains, an ATP pyrophosphatase (ATPPase) domain, and two dimerization domains (Fig. 1a), while the GATase domain is composed of a single structural domain.

GATase domain

The GATase domain is composed of a central β-sheet surrounded by mainly α-helices, comprising the catalytic triad Cys104, His190, and Glu192 (Fig. 1c). A DALI search [23] of this domain reveals similarity to other GATase domains of amidotransferases with the GATase domain of *Ec*GMPS as the closest structural homolog with a root-mean-square deviation (r.m.s.d.) of 1.5 Å for 175 amino acids. Currently, there is no experimental structural information of glutamine binding to the GATase domain of a GMPS, but based on homology, it is expected to bind glutamine similarly as anthranilate synthase [24]. The ammonium generated by the GATase domain is utilized by the ATPPase domain located near the GATase domain in the structure (Fig. 1a). The active site of the GATase domain where the ammonia is generated is situated ca 40 Å away from the bound XMP to the synthetase domain, making it necessary for ammonia to be transferred by an unknown mechanism to the second active site.

ATPPase domain

The ATPPase sub-domain of hGMPS is composed of a five-stranded parallel β-sheet sandwiched between nine α-helices (Fig. 1b). The substrate XMP is bound to this sub-domain. Residues 368–408 form a lid-like region (in the following referred to as the lid) closing in over the active site (Fig. 1b and d). One of the sulfate ions (S1) found in the structure is bound to a conserved phosphate binding loop composed of residues 244–250 and occupying the binding site for the phosphate moiety of ATP in the structure of *Ec*GMPS (PDB ID: 1GPM) [25].

Oligomerization

Since hGMPS possesses two dimerization subdomains, the dimer organization is completely different from its bacterial counterparts. Of the total surface area, ~20% (~10,000 Å [2]) is buried upon formation of the dimer. Also, for eukaryotic sequences, the dimer displays a higher level of conservation around the dimer interface (Fig. 2a). There are fewer conserved residues in the D1 subdomain except around the β-hairpin, which is highly conserved (Fig. 2b). Since the crystal structure supports the notion that hGMPS is a dimeric enzyme,

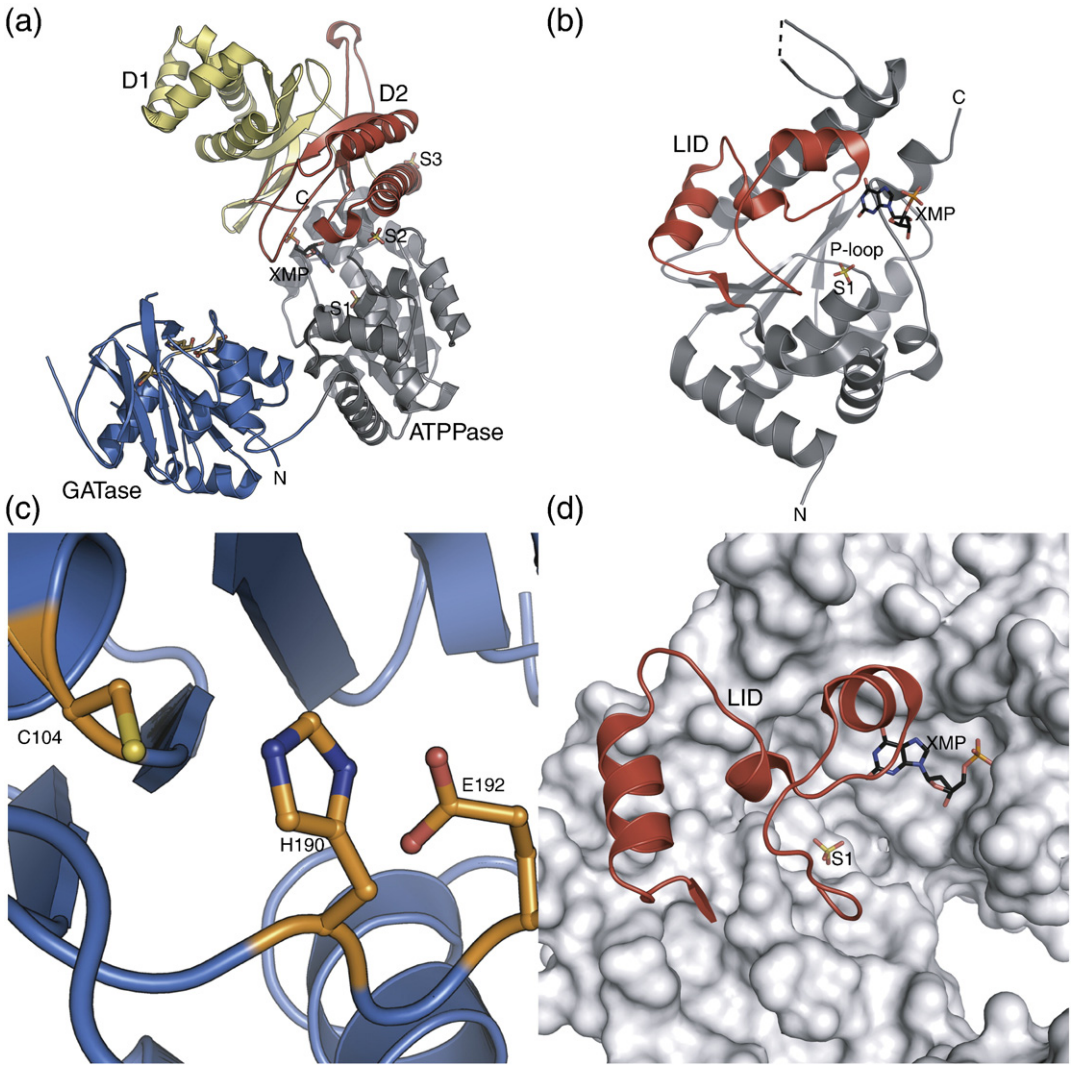

Fig. 1. Structure of hGMPS. (a) The subunit structure of GMPS containing the GATase domain (blue), ATPPase sub-domain (gray), and dimerization sub-domain 1 (D1) (yellow) and 2 (D2) (red). The catalytic triad of the GATase (residues: Cys104, His190, and Glu192) are shown as yellow sticks. XMP and sulfate ions bound are also shown as sticks. (b) ATPPase sub-domain of hGMPS. The LID region consisting of residues 368–408 is colored red. The ATPPase domain is colored gray. (c) Close-up view of the catalytic triad of the GATase domain; residues are shown in sticks in orange. (d) LID region. The LID region is displayed in cartoon and the other domains of hGMPS are shown with surface, colored red and white, respectively.

in contrast with earlier data [18,21], analytical gel filtration was performed to elucidate the oligomeric state of hGMPS in solution. A large peak corresponding to a monomer was observed when size-exclusion chromatography was run in the presence of XMP + Mg, ATP + Mg, XMP + ATP + Mg, and without substrates. However, a small additional peak was observed prior to monomer peak with a size corresponding to approximately a dimer (Fig. 2c), indicating a small dimer population in solution. To further investigate the oligomeric state, we performed cross-linking experiments in the presence of glutamine analogs DON and azaserine, known to bind to the glutamine binding site of the GATase domain [26]. These experiments were performed together with XMP, ATP, and Mg^{2+} to trap an active state of the protein. Dimerization was induced in the presence of DON, while azaserine or the apo form of GMPS did not form dimers (Fig. 2d). This suggests that the active form of hGMPS, containing all co-substrates, could be a dimer.

Dimerization sub-domains

Mammalian GMPSs contain a long insert that stretches from residue 450 to residue 578 constituting the D1 sub-domain, which is absent in bacterial and archaeal counterparts (Fig. 3). This sub-domain is built up by an anti-parallel three-stranded β-sheet, where the middle β-strand stretches out to form a β-

hairpin. The β-sheet is flanked by five α-helices. In the structure, this sub-domain is involved in dimerization and substrate binding (Fig. 1a). Interestingly, the β-hairpin (Ile514–Tyr528) stretches into the XMP binding site of the other subunit in the dimer, where Arg524 from the β-hairpin in subunit A and Asp522 from the β-hairpin in subunit B interact with each other and with the phosphate moiety of XMP bound to subunit A (Fig. 4a). The last 115 residues of hGMPS (579–693) form a second dimerization sub-domain, the D2 sub-domain. The fold of the two dimerization sub-domains D1 and D2 is similar and superposition of the two sub-domains gives an r.m.s.d. of 2.2 Å for 73 C^{α}.

Substrate binding

The XMP molecule is bound in the active site located in between the ATPPase sub-domain and the D2 sub-domain of the same subunit (Fig. 1a). The lid is closing in over the active site and the xanthine base is wedged between a conserved Pro-rich region (residues 438–441) and a loop containing residues 383–385 of the lid. Arg337 is the key residue in discriminating XMP from

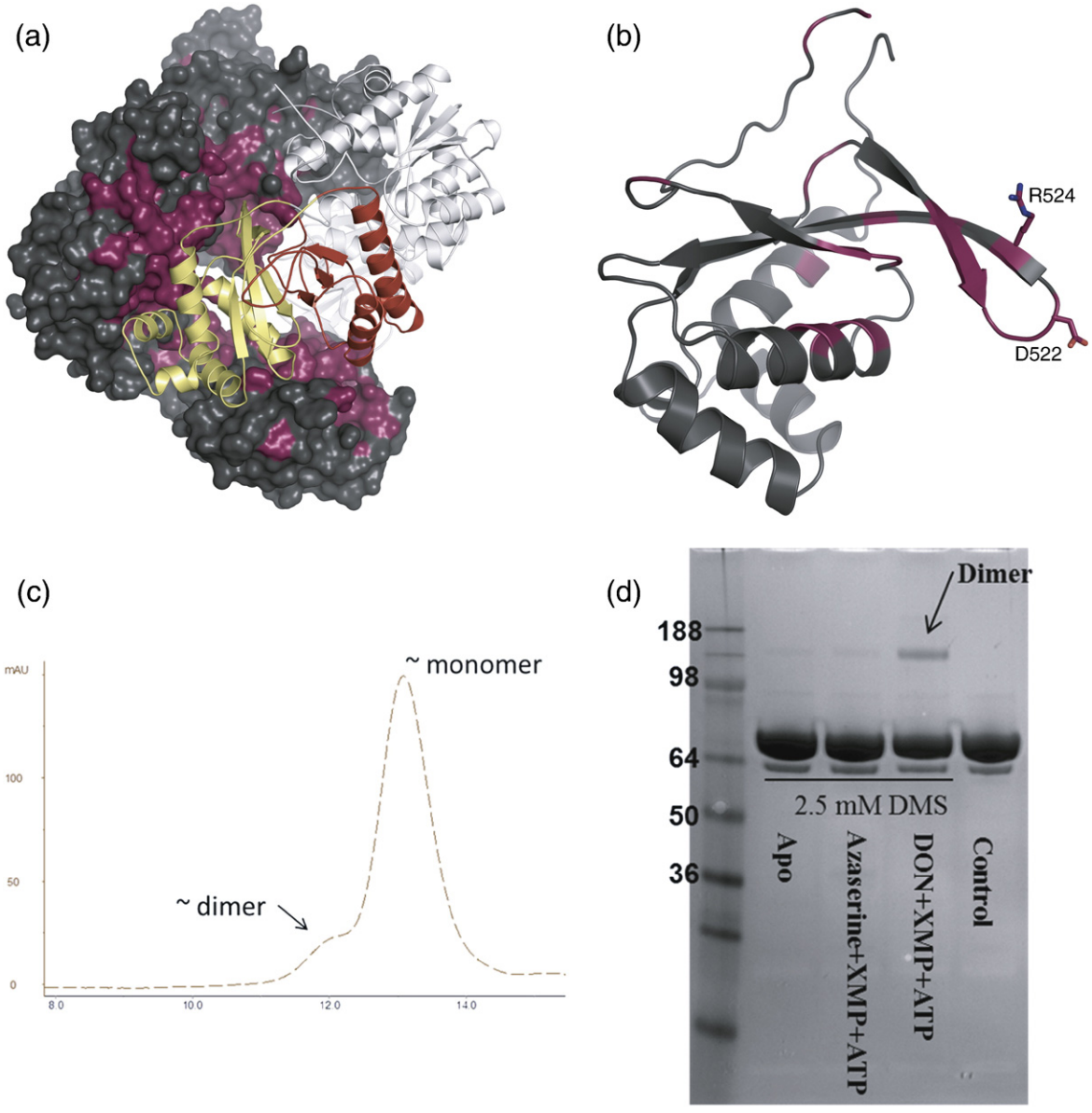

Fig. 2. Sequence conservation for hGMPS. (a) hGMPS dimer using surface representation for subunit A and cartoon representation for subunit B colored white, yellow (D1), and red (D2). Highly conserved residues are colored purple and the remaining residues are in dark gray. (b) Cartoon representation of the D1 sub-domain showing side chains Asp522 and Arg524 in sticks; same coloring scheme as in (a). (c) Analytical size-exclusion chromatography for full-length hGMPS. (d) SDS-PAGE showing the dimer formation in the cross-linking experiment.

other purine monophosphates, making specific interactions to O6 and N7 of the xanthine base (Fig. 4a). The conformation of this arginine is stabilized by interactions from the carboxylate group of the C-terminus of the protein (Fig. 4a). The ribose moiety makes well-defined interactions with Gln610 and Glu691 (Fig. 4a). The phosphate moiety of XMP interacts with residues Arg524, Lys685, Thr690, Glu691, and Asp522 from the B subunit (Fig. 4b). The hydrogen bonding of a carboxylate residue (Glu691) with the ribose hydroxyl is a common motif for specific recognition of ribonucleotides [27].

The high concentration of ammonium sulfate in the crystallization condition likely explains why the AMPPNP does not bind to the ATP binding site in the crystal. The sulfate S1 bound in the phosphate binding loop (Fig. 1b) makes hydrogen bonds to the side chain of Ser244 and main chain of Ser249.

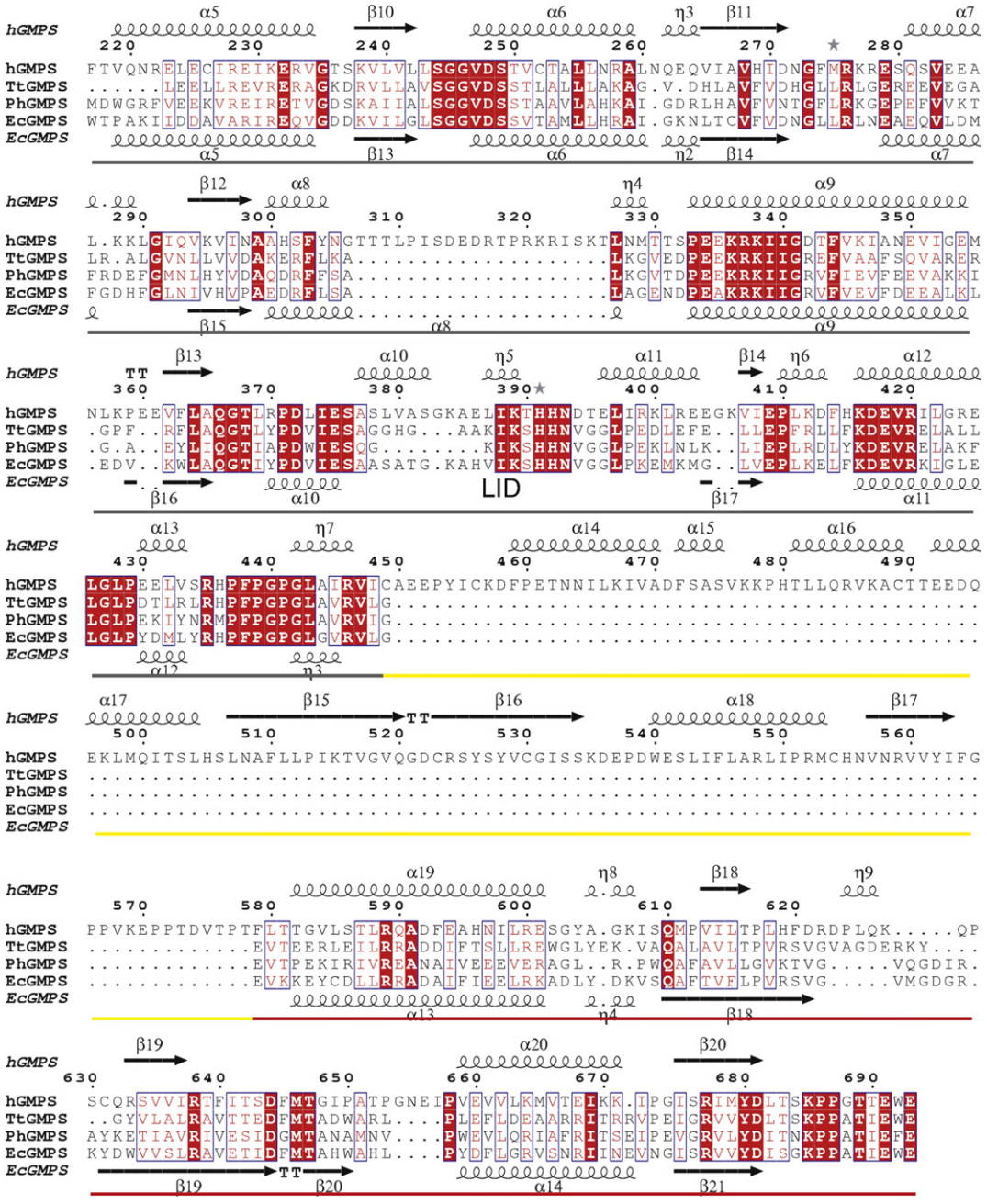

Fig. 3. Structure-based sequence alignment of the GMPS synthetase domains from human, *Tt*GMPS, *Ph*GMPS, and *EcGMPS*. Sub-domains are color coded as in Fig. 1a. The LID is marked in the alignment. Secondary-structure elements are shown for hGMPS and *Ec*GMPS above and below the alignment.

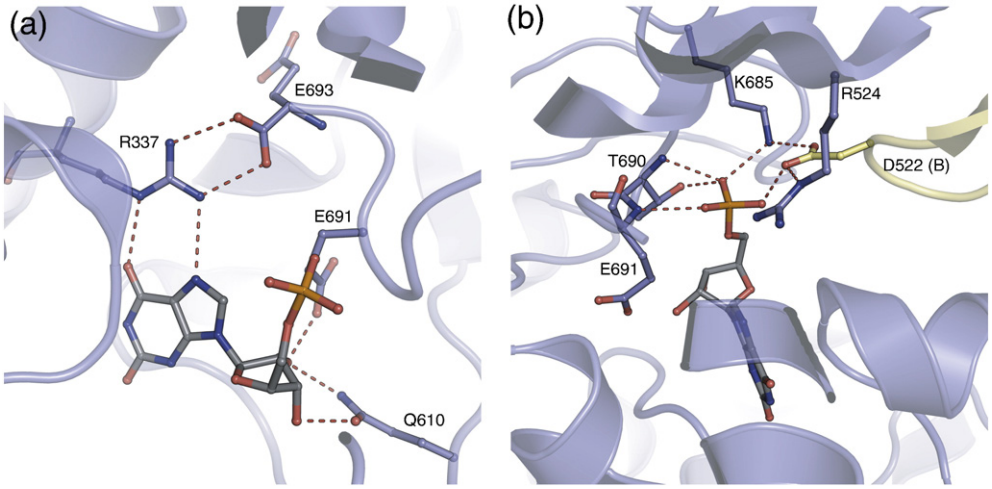

Fig. 4. Binding of XMP to hGMPS. (a) Interactions with the xanthine base and ribose moiety of XMP. Residues involved in binding and XMP are shown in sticks colored slate blue and gray. (b) Interactions with the phosphate moiety of XMP. Residues involved in binding and XMP are shown with sticks using the same coloring. Asp522 from the other subunit is colored yellow.

A second sulfate ion (S2) is bound ~12 Å from the ribose moiety of XMP. S2 is located in a pocket between the D1 sub-domain and the ATPPase sub-domain, close to the Pro-rich region lining the xanthine base (Fig. 1a). Several positively charged residues are lining the pocket where the sulfate ion is bound. It is possible that this is a binding site for a regulatory phosphate-containing molecule although evidence for this remains to be provided.

Comparison with prokaryotic GMPSs

Comparison of the structures of the bacterial and archaeal GMPSs with the hGMPS reveals that the eukaryotic enzyme has several unique attributes. D1 sub-domain in hGMPS is absent in bacterial proteins, but the other domains have a very similar orientation (Fig. 5a). The hGMPS dimer is more tightly packed (Fig. 5b), whereas the overall shape of the bacterial and archaeal GMPS dimer is more open (Fig. 5c). *Ec*GMPS forms a dimer using its dimerization sub-domain that is built up by a mixed β-sheet (Fig. 5c) [1]. Comparing the dimerization sub-domain from prokaryotic GMPSs with the D1 and D2 sub-domains of hGMPS reveals strikingly similar polypeptide folds of these domains (Fig. 6a) with an r.m.s.d. of 1.9–2.4 Å according to the DALI server [23]. The orientation of D1 and D2 sub-domains in the hGMPS is very similar to the dimer formed by the sub-domain in the *Ec*GMPS with an r.m.s.d. of 1.2 Å over 101 residues (Fig. 6b).

Multiple sequence alignment comparing mammalian, bacterial, and archaeal sequences reveals a region in the unique human D1 sub-domain that is

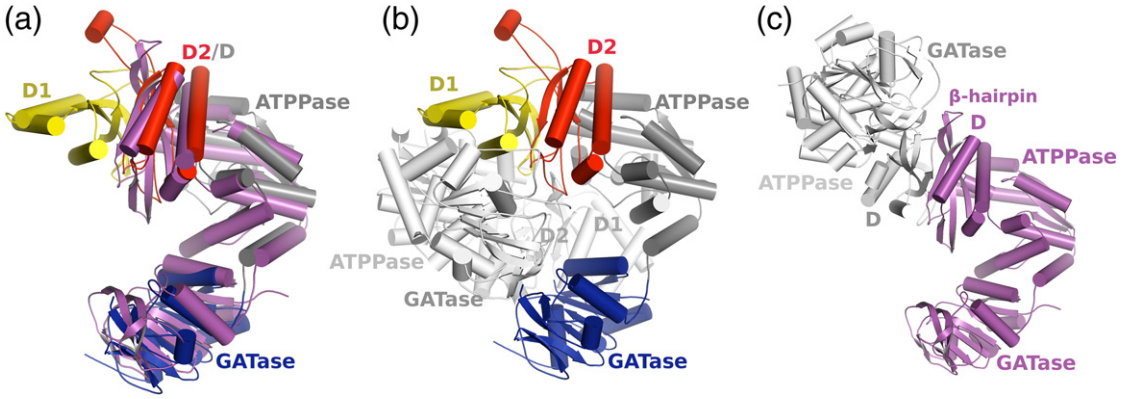

Fig. 5. Subunit compositions of different GMPSs. (a) Superposition of hGMPS and *Ec*GMPS (magenta) monomers. The domains of GMPS are colored as in Fig. 1: GATase domain, blue; ATPPase sub-domain, gray; and dimerization sub-domains 1 and 2 (D1 and D2), yellow and red, respectively. (b) Dimer of hGMPS with the second monomer shown in light gray. (c) *Ec*GMPS with the second monomer shown in light gray.

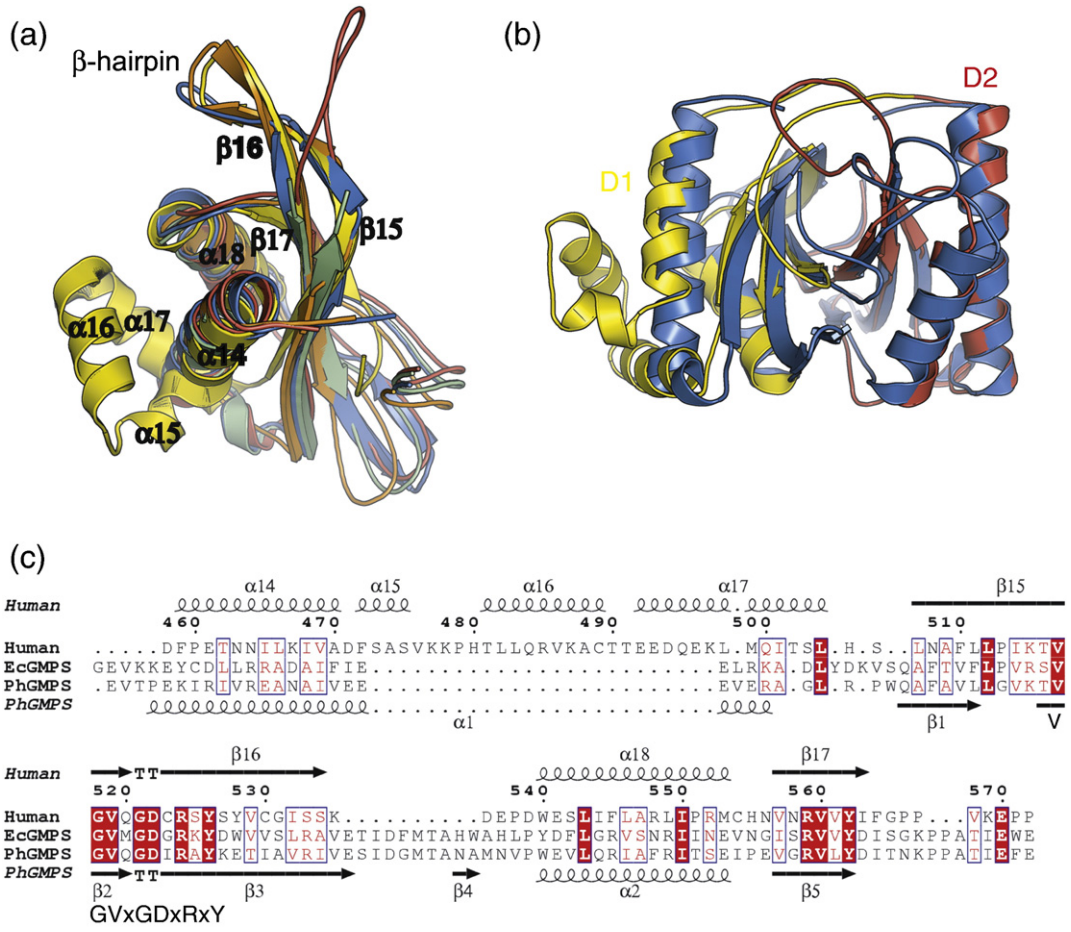

Fig. 6. Comparison of dimerization domains. (a) Superposition of the dimerization sub-domains D1 (yellow) and D2 (red) of hGMPS, *Ec*GMPS (blue), *Tt*GMPS (green), and *Ph*GMPS (orange). (b) Superposition of hGMPS D1 (yellow) and D2 (red) sub-domains and the two dimerization sub-domains of *Ec*GMPS dimer (blue). (c) Structure-based sequence alignment of human D1 with dimerization sub-domains of *Ec*GMPS and *Ph*GMPS. Secondary-structure elements are shown for hGMPS and *Ph*GMPS above and below the alignment.

highly conserved to a part of the dimerization sub-domain of bacterial proteins. This region has the consensus sequence Val-Gly-Val-x-Gly-Asp-x-Arg-x-Tyr (Fig. 6c) and interestingly it is not present in the D2 domain of hGMPS, which in the monomer structure superposes with the dimerization domain of EcGMPS (Fig. 5a). This conserved region of the dimerization domain is also involved in binding of XMP. In hGMPS, residues Asp522 and Arg524 are interacting not only with each other from the opposite subunit but also with the phosphate moiety of XMP (Fig. 4b). In prokaryotic GMPSs, this β-hairpin is either unstructured or taking slightly different conformations, indicating flexibility (Figs. 6a and 5c). In the *Ec*GMPS, the main chain of the Asp462 corresponding to Asp522 in hGMPS is situated 34 Å away from the phosphate bound to the XMP binding site in the same subunit. However, the distance to the phosphate in the other subunit in the dimer is 18 Å (Fig. 5c). When the human D1 domain is superimposed on the dimerization domain of prokaryotic GMPSs, it becomes clear that the β-hairpin ends up close to the phosphate moiety of XMP from the other subunit of the dimer. This indicates that the conserved aspartic acid may have an important role in prokaryotes as well.

Discussion

hGMPS possesses a second dimerization sub-domain not present in bacterial and archaeal GMPSs. Duplication of the dimerization domain mimics the dimer seen in bacterial enzymes, but the distance and orientation between the two active sites in hGMPS and *Ec*GMPS are similar (Fig. 5) [1]. There appears to be an equilibrium with the monomeric and dimeric form of the enzyme, and under the tested conditions, the enzyme is mostly a monomer in solution. It is not clear when and how the dimerization occurs, but it is enhanced by substrate binding. In the crystal, the dimeric form could be stabilized by high concentration and by the nonphysiological precipitant condition.

Binding of the substrate induces dimer formation leading to an ordered lid domain, which could play a role in cooperation of the enzymatic activities and perhaps in transfer of the ammonia.

The long distance between the active sites and the lack of a clear route for ammonia transfer indicate domain rearrangements during reaction as for the *Ec*GMPS [1]. In contrast to the EcGMPS, there is also a possibility of an intermonomer transfer of ammonia through the center of the globular oligomer due to unique oligomeric packing observed in the crystal structure. However, as the orientation of the GATase and ATPPase domains is similar in both enzymes (Fig. 5), it seems likely that the mechanism of the ammonia transfer would be also similar. An intriguing possibility is that the LID domain that has been disordered in previous crystal structures could contribute to the cooperation of the active site and perhaps to the transfer of ammonia.

In *Ec*GMPS, 22 residues of the lid are flexible and believed to be stabilized upon XMP binding [1]. In the case of *Tt*GMPS (PDB ID: 2YWC), part of the lid is flexible albeit XMP binding, indicating that bacterial GMPSs may require both XMP and ATP for lid closure. In hGMPS, the D1 sub-domain from the other subunit in the dimer is partly stabilizing the lid. The lid in hGMPS is ordered and closes in over both the ATP and XMP binding sites. The observed conformation might be the conformation present during catalysis. Earlier studies of hGMPS have revealed a monomeric enzyme using density gradient centrifugation [18,21]. Positive cooperativity was observed for the substrate XMP and it was speculated that there would be a second XMP binding site in hGMPS [18,21]. We observed a potential ligand binding site marked by S2 located ~12 Å from the ribose moiety of XMP. S2 is located in a pocket between the D2 sub-domain and the ATPPase sub-domain, close to the Pro-rich region lining the xanthine base (Fig. 1a). This cavity is lined by several residues appropriate for binding both a phosphate and a ribose moiety. However, we have not been able to obtain evidence that this is indeed an allosteric site where, for example, XMP could bind. Another, more likely explanation for the observed positive cooperativity would be that a dimeric protein is induced by substrate binding. This is supported by the interactions of XMP and residues from the other subunit in the dimer, indicating cross-talk between the subunits. In addition, interactions between the lid and the D1 sub-domain of the second subunit could contribute to cross-talk within the dimer. In solution, we observed that hGMPS was predominantly a monomer with only a small population of dimers. The cross-linking experiments suggest that XMP, ATP, and glutamine are needed to induce dimer formation in solution.

Asp522 and Arg524 are part of the conserved motif in the D1 sub-domain. The fact that Asp522 stretches in from the other subunit towards the phosphate moiety is surprising, and the carboxylate phosphate interaction appears unfavorable. The temperature factors in the tip of the β-hairpin are higher than those of the surrounding residues. In the bacterial counterpart, the conserved aspartic acid is located ~18 Å from the XMP binding site in the other subunit and ~34 Å away in the same subunit. In *Tt*GMPS, the tip of the β-hairpin is flexible despite XMP binding. The superposition of the human D1 sub-domain on prokaryotic GMPSs indicates that the β-hairpin may become ordered and swings in towards the XMP molecule upon substrate binding. One aspect of this conserved aspartic acid could be to facilitate product release. In the case of hGMPS, it might play a part in dimer formation, bringing the two subunits together with interactions between Asp522 and Arg524.

Since numerous enzymes in the nucleotide metabolism display an increased activity in proliferating cells, they might be attractive cancer targets [5]. Many of the drugs targeting enzymes in the nucleotide metabolism act on a broader range of enzymes, which might add potency and might also be the cause of excessive toxicity [28]. Structural information on these enzymes is therefore valuable in efforts directed at developing new, more selective drugs. Information on structural differences between human and pathogen enzymes might also assist in the development of novel antibiotics targeting the nucleotide metabolism. In times of increasing bacterial resistance, there is as well a growing need for new anti-bacterial agents [29]. Therefore, the structural information provided in the present work might be directly useful in therapeutic development.

Materials and Methods

Cloning

The GMPS gene clone was obtained from the National Institutes of Health's Mammalian Gene Collection (accession no. BC012178). The sequence encoding residues 20–693 and 1–693 were amplified by PCR and inserted into pNIC28-Bsa4 vector by ligation-independent cloning. Constructs included an N-terminal tag containing a 6-His sequence (MHHHHHHSSGVDLGTENLYFQSM). For expression, the pNIC-Bsa4 containing the insert was transformed into *E. coli* BL21(DE3) gold pRARE strain and stored at −80 °C for further use.

Protein expression

Cells from a glycerol stock were grown in 60 mL of TB supplemented with 8 g/L glycerol, 100 μg/mL kanamycin, and 34 μg/mL chloramphenicol at 37 °C overnight. The overnight culture (60 mL) was used to inoculate three flasks with 1.5 L of TB each, supplemented with 50 μg/mL kanamycin and approximately 0.5 mL of Dow Corning anti-foam RD emulsion 63213 4D (BDH Silicone Products).

The cultures were grown at 37 °C until OD_{600} reached ~2. The flasks were down-tempered to 18 °C over a period of 30 min before target expression was induced by addition of 0.5 mM IPTG. Expression was allowed to continue overnight and cells were harvested the following morning by centrifugation (4400***g***, 20 min, 4 °C) and stored at −80 °C.

Protein purification

The frozen cell pellet was re-suspended in lysis buffer (100 mM Hepes, 500 mM NaCl, 10% glycerol, 10 mM imidazole, and 0.5 mM TCEP, pH 8.0), supplemented with 0.25 mg of lysozyme, 1000 U Benzonase (Merck), and one tablet of Complete EDTA-free protease inhibitor (Roche Applied Science). Cells were disrupted by sonication (Vibra-Cell, Sonics) at 80% amplitude for 3 min effective time (pulsed 4 s on, 4 s off), and cell debris was removed by centrifugation (49,100***g***, 20 min, 4 °C). The supernatant was decanted and filtered through a 0.45-μm flask filter. Purification of the protein was performed as a two-step process on an ÄKTAxpress system (GE Healthcare). Prior to purification, columns were equilibrated using lysis buffer and gel-filtration buffer (20 mM Hepes, 300 mM NaCl, 10% glycerol, and 2 mM TCEP, pH 7.5). The protein sample was divided into three equal parts and each was loaded onto a Ni-charged 1-mL HiTrap Chelating HP (GE Healthcare). The IMAC columns were washed with wash buffer 1 containing (20 mM Hepes, 500 mM NaCl, 10% glycerol, 10 mM imidazole, and 0.5 mM TCEP, pH 7.5) followed by wash buffer 2 containing (20 mM Hepes, 500 mM NaCl, 10% glycerol, 25 mM imidazole, and 0.5 mM TCEP, pH 7.5). Bound protein was eluted from the IMAC columns with IMAC elution buffer (20 mM Hepes, 500 mM NaCl, 10% glycerol, 500 mM imidazole, and 0.5 mM TCEP, pH 7.5) and automatically loaded onto a HiLoad 16/60 Superdex 200 Prep Grade (GE Healthcare) gel-filtration column. Fractions containing the target protein were pooled. A similar protocol was used for the expression and purification of the full-length GMPS. The protein was subsequently concentrated using a Centricon centrifugal filter device with 30,000 NMWL (Millipore) to 13.0 mg/mL (truncated enzyme) and 26 mg/mL (full-length enzyme) and stored at −80 °C. The identity of the protein was confirmed by mass spectrometry [30].

Analytical gel filtration

Analytical gel filtration was performed on an Äkta Purifier using a Superdex 200 10/300 column equilibrated with 20 mM Hepes, 300 mM NaCl, 10% glycerol, and 2.0 mM TCEP, pH 7.5. GMPS were run in its apo form, with 1 mM XMP and 10 mM $MgCl_2$, with 1 mM ATP and 10 mM $MgCl_2$ and 1 mM XMP, or with 1 mM ATP and 10 mM $MgCl_2$. For each run, 300 μg of the full-length GMPS was used. The samples were incubated for 30 min to 1 h before each gel-filtration run.

Cross-linking assay

Cross-linking experiment with full-length hGMPS was performed using dimethyl suberimidate. The reaction mixture contained GMPS at a concentration of 1 mg/mL with 5 mM $MgCl_2$ in gel-filtration buffer. This mixture was used either alone or with the combinations of 1 mM XMP, 1 mM ATP, 5 mM $MgCl_2$, and 1 mM of glutamine analogs DON or azaserine. After 3 h in room temperature, the reaction was quenched by addition of 1 M Tris, pH 8. Cross-linking was then analyzed on SDS-PAGE to visualize dimer formation.

Crystallization, data collection, and structure determination

Crystals of hGMPS (residues 20–693) were obtained by the sitting drop vapor diffusion method using 96-well plates by mixing 0.2 μL of the protein solution (12 mg/mL + 5 mM XMP + 5 mM AMPPNP + 10 mM $MgCl_2$) with 0.1 μL of the well solution consisting of 0.1 M sodium acetate trihydrate, pH 5.2, 1.6 M ammonium sulfate, and 0.2 M sodium chloride at room temperature. Crystals typically appeared after 2–5 days and were mounted in a rayon loop and transferred to a cryo-protectant solution containing 0.1 M sodium acetate trihydrate, pH 5.2, 1.6 M ammonium sulfate, 0.3 M sodium chloride, and 25% glycerol. The crystal was briefly soaked in the cryo-protectant solution before being flash frozen in liquid nitrogen. Diffraction data were collected at BESSY beam line BL14-2 and processed with XDS

Table 1. Data and refinement statistics

	GMPS
Beam line	BL14-2 (BESSY)
Wavelength (Å)	0.97968
Space group	$P2_12_12_1$
Resolution (Å)	20–2.5 (2.56–2.50)
Cell dimensions	
a, *b*, *c* (Å)	98.52, 123.42, 127.96
R_{merge}	0.094 (0.587)
$I/\sigma(I)$	18.9 (4.12)
Completeness (%)	99.7 (100)
Redundancy	7.7 (7.8)
Refinement	
No. of reflections	51,746
R_{work}[a]/R_{free}[b]	0.203/0.256
No. of atoms	
Protein	10,043
XMP	48
Water	125
Other	30
B-factors (Å^2)	
Protein	36.8
XMP	23.6
Water	31.3
Other	69.9
r.m.s.d.	
Bond lengths (Å)	0.009
Bond angles (°)	1.2
Ramachandran plot (%)[c]	
Favored regions	98
Additionally allowed regions	2

$R_{merge} = \sum_i |I_i - \langle I \rangle| / \sum \langle I \rangle$, where I is an individual intensity measurement and $\langle I \rangle$ is the average intensity for this reflection with summation over all data.

Values for the highest-resolution shell are shown in parentheses.

[a] R_{work} is defined as $\sum ||F_{obs}| - |F_{calc}|| / \sum |F_{obs}|$, where F_{obs} and F_{calc} are observed and calculated structure-factor amplitudes, respectively.

[b] R_{free} is the *R*-factor for the test set (5% of the data).

[c] According to MolProbity [31].

(Table 1) [32]. For molecular replacement, separate searches were done for each domain using PHASER [33]. As search models, the GATase domain of hGMPS (PDB ID: 2VPI) and the synthetase domain (195–503) of GMPS from *T. thermophilus* (PDB ID: 2YWC) were used. The initial model was then automatically built using PHENIX autobuild [34]. Final cycles of model building and refinement were performed in Coot [35] and REFMAC5 [36]. All data collection and refinement statistics are shown in Table 1.

Structure alignments and analysis

Superposition of the structures were done with Coot [35] using the secondary-structure matching-based algorithm [37]. All the figures were generated with PyMOL [38]. Structural sequence alignment was made using STRAP (PDB IDs: 2VXO, 1GPM, 2YWC, and 3A4I) [39]. The multiple alignments were carried out using ClustalW2 [40] and visualized using ESPript [41]. Surface areas were calculated using the PISA server [42]. To visualize the level of conservation, we used a multiple alignment with 41 eukaryotic sequences selected by the ConSurf server [43,44].

Accession number

The coordinates and structure factors have been deposited to the PDB with the accession code 2VXO.

Acknowledgements

This work was supported by grants from the Swedish Research Council and the Swedish Cancer Society (P.N.). We acknowledge BESSY for synchrotron radiation facilities and we would like to thank the staff for assistance in using beam lines BL14-2. The Structural Genomics Consortium is a registered charity (number 1097737) that receives funds from the Canadian Institutes for Health Research, the Canadian Foundation for Innovation, Genome Canada through the Ontario Genomics Institute, GlaxoSmithKline, Karolinska Institutet, the Knut and Alice Wallenberg Foundation, the Ontario Innovation Trust, the Ontario Ministry for Research and Innovation, Merck & Co., Inc., the Novartis Research Foundation, the Swedish Agency for Innovation Systems, the Swedish Foundation for Strategic Research, and the Wellcome Trust.

Received 21 April 2013;
Received in revised form 20 June 2013;
Accepted 21 June 2013
Available online 28 June 2013

Keywords:
GMP synthetase;
crystal structure;
amidotransferase;
substrate specificity;

This is an open-access article distributed under the terms of the Creative Commons Attribution-NonCommercial-No Derivative Works License, which permits non-commercial use, distribution, and reproduction in any medium, provided the original author and source are credited.

Present addresses: M. Welin, SARomics Biostructures AB, Medicon Village, SE-223 81 Lund, Sweden; L. Lehtiö, Biocenter Oulu, Department of Biochemistry, University of Oulu, P.O. Box 3000, FIN-90014 Oulu, Finland; M. Hammarström, Pfizer Health AB, Box 108, 64522 Strängnäs, Sweden; S. Gräslund, Structural Genomics Consortium, University of Toronto, 101 College Street, Toronto, ON M5G1L7, Canada.

Abbreviations used:
GMP, guanine monophosphate; XMP, xanthine monophosphate; GMPS, GMP synthetase; GATase, glutaminase; hGMPS, human GMPS; *Ec*GMPS, *Escherichia coli* GMPS; *Ph*GMPS, *Pyrococcus horikoshii* OT3 GMPS; *Tt*GMPS, *Thermus thermophilus* GMPS; ATPPase, ATP pyrophosphatase; DON, 6-diazo-5-oxo-L-norleucine; PDB, Protein Data Bank.

References

[1] Tesmer JJ, Klem TJ, Deras ML, Davisson VJ, Smith JL. The crystal structure of GMP synthetase reveals a novel catalytic triad and is a structural paradigm for two enzyme families. Nat Struct Biol 1996;3:74–86.
[2] Fukuyama TT. Formation of an adenyl xanthosine monophosphate intermediate by xanthosine 5′-phosphate aminase and its inhibition by psicofuranine. J Biol Chem 1966;241:4745–9.
[3] Von der Saal W, Crysler CS, Villafranca JJ. Positional isotope exchange and kinetic experiments with *Escherichia coli* guanosine-5′-monophosphate synthetase. Biochemistry 1985;24:5343–50.
[4] Raushel FM, Thoden JB, Holden HM. The amidotransferase family of enzymes: molecular machines for the production and delivery of ammonia. Biochemistry 1999;38:7891–9.
[5] Weber G. Biochemical strategy of cancer cells and the design of chemotherapy: G.H.A. Clowes Memorial Lecture. Cancer Res 1983;43:3466–92.
[6] Weber G, Nakamura H, Natsumeda Y, Szekeres T, Nagai M. Regulation of GTP biosynthesis. Adv Enzyme Regul 1992;32:57–69.
[7] Lui MS, Kizaki H, Weber G. Biochemical pharmacology of acivicin in rat hepatoma cells. Biochem Pharmacol 1982;31:3469–73.
[8] Hirst M, Haliday E, Nakamura J, Lou L. Human GMP synthetase. Protein purification, cloning, and functional expression of cDNA. J Biol Chem 1994;269:23830–7.
[9] Achleitner E, Lui MS, Weber G. Inactivation by acivicin of rat brain CTP and GMP synthetases and depression of CTP and GTP concentrations. Adv Enzyme Regul 1985;24:225–32.
[10] Kaufman ER. Isolation and characterization of a mutant Chinese hamster cell line resistant to the glutamine analog 6-diazo-5-oxo-L-norleucine. Somat Cell Mol Genet 1985;11:1–10.

[11] Hedstrom L. IMP dehydrogenase: structure, mechanism, and inhibition. Chem Rev 2009;109:2903–28.
[12] Van der Knaap JA, Kumar BRP, Moshkin YM, Langenberg K, Krijgsveld J, Heck AJR, et al. GMP synthetase stimulates histone H2B deubiquitylation by the epigenetic silencer USP7. Mol Cell 2005;17:695–707.
[13] Long H, Cameron S, Yu L, Rao Y. De novo GMP synthesis is required for axon guidance in *Drosophila*. Genetics 2006;172: 1633–42.
[14] Faesen AC, Dirac AMG, Shanmugham A, Ovaa H, Perrakis A, Sixma TK. Mechanism of USP7/HAUSP activation by its C-terminal ubiquitin-like domain and allosteric regulation by GMP-synthetase. Mol Cell 2011;44:147–59.
[15] Zalkin H, Truitt CD. Characterization of the glutamine site of *Escherichia coli* guanosine 5′-monophosphate synthetase. J Biol Chem 1977;252:5431–6.
[16] Bhat JY, Shastri BG, Balaram H. Kinetic and biochemical characterization of *Plasmodium falciparum* GMP synthetase. Biochem J 2008;409:263–73.
[17] Abbott JL, Newell JM, Lightcap CM, Olanich ME, Loughlin DT, Weller MA, et al. The effects of removing the GAT domain from *E. coli* GMP synthetase. Protein J 2006;25:483–91.
[18] Nakamura J, Lou L. Biochemical characterization of human GMP synthetase. J Biol Chem 1995;270:7347–53.
[19] McConkey GA. *Plasmodium falciparum*: isolation and characterisation of a gene encoding protozoan GMP synthase. Exp Parasitol 2000;94:23–32.
[20] Maruoka S, Horita S, Lee WC, Nagata K, Tanokura M. Crystal structure of the ATPPase subunit and its substrate-dependent association with the GATase subunit: a novel regulatory mechanism for a two-subunit-type GMP synthetase from *Pyrococcus horikoshii* OT3. J Mol Biol 2010;395:417–29.
[21] Lou L, Nakamura J, Tsing S, Nguyen B, Chow J, Straub K, et al. High-level production from a baculovirus expression system and biochemical characterization of human GMP synthetase. Protein Expr Purif 1995;6:487–95.
[22] Mouilleron S, Golinelli-Pimpaneau B. Conformational changes in ammonia-channeling glutamine amidotransferases. Curr Opin Struct Biol 2007;17:653–64.
[23] Holm L, Sander C. Protein structure comparison by alignment of distance matrices. J Mol Biol 1993;233:123–38.
[24] Spraggon G, Kim C, Nguyen-Huu X, Yee MC, Yanofsky C, Mills SE. The structures of anthranilate synthase of *Serratia marcescens* crystallized in the presence of (i) its substrates, chorismate and glutamine, and a product, glutamate, and (ii) its end-product inhibitor, L-tryptophan. Proc Natl Acad Sci USA 2001;98:6021–6.
[25] Bork P, Koonin EV. A P-loop-like motif in a widespread ATP pyrophosphatase domain: implications for the evolution of sequence motifs and enzyme activity. Proteins 1994;20:347–55.
[26] Chittur SV, Klem TJ, Shafer CM, Davisson VJ. Mechanism for acivicin inactivation of triad glutamine amidotransferases. Biochemistry 2001;40:876–87.
[27] Welin M, Nordlund P. Understanding specificity in metabolic pathways—structural biology of human nucleotide metabolism. Biochem Biophys Res Commun 2010;396:157–63.
[28] Van Rompay AR, Johansson M, Karlsson A. Substrate specificity and phosphorylation of antiviral and anticancer nucleoside analogues by human deoxyribonucleoside kinases and ribonucleoside kinases. Pharmacol Ther 2003; 100:119–39.
[29] Alekshun MN, Levy SB. Molecular mechanisms of antibacterial multidrug resistance. Cell 2007;128:1037–50.
[30] Sundqvist G, Stenvall M, Berglund H, Ottosson J, Brumer H. A general, robust method for the quality control of intact proteins using LC-ESI-MS. J Chromatogr B Analyt Technol Biomed Life Sci 2007;852:188–94.
[31] Lovell SC, Davis IW, Arendall WB, De Bakker PI, Word JM, Prisant MG, et al. Structure validation by Calpha geometry: phi, psi and Cbeta deviation. Proteins 2003;50:437–50.
[32] Kabsch W. Automatic processing of rotation diffraction data from crystals of initially unknown symmetry and cell constants. J Appl Crystallogr 1993;26:795–800.
[33] McCoy AJ, Grosse-Kunstleve RW, Storoni LC, Read RJ. Likelihood-enhanced fast translation functions. Acta Crystallogr Sect D Biol Crystallogr 2005;61:458–64.
[34] Adams PD, Grosse-Kunstleve RW, Hung LW, Ioerger TR, McCoy AJ, Moriarty NW, et al. PHENIX: building new software for automated crystallographic structure determination. Acta Crystallogr Sect D Biol Crystallogr 2002;58:1948–54.
[35] Emsley P, Cowtan K. Coot: model-building tools for molecular graphics. Acta Crystallogr Sect D Biol Crystallogr 2004;60:2126–32.
[36] Murshudov GN, Vagin AA, Dodson EJ. Refinement of macromolecular structures by the maximum-likelihood method. Acta Crystallogr Sect D Biol Crystallogr 1997;53: 240–55.
[37] Krissinel E, Henrick K. Secondary-structure matching (SSM), a new tool for fast protein structure alignment in three dimensions. Acta Crystallogr Sect D Biol Crystallogr 2004;60: 2256–68.
[38] DeLano WL. The PyMOL Molecular Graphics System. Palo Alto, CA, USA: DeLano Scientific; 2002. http://www.pymol.org.
[39] Gille C, Frömmel C. STRAP: editor for STRuctural Alignments of Proteins. Bioinformatics 2001;17:377–8.
[40] Larkin MA, Blackshields G, Brown NP, Chenna R, McGettigan PA, McWilliam H, et al. Clustal W and Clustal X version 2.0. Bioinformatics 2007;23:2947–8.
[41] Gouet P, Robert X, Courcelle E. ESPript/ENDscript: Extracting and rendering sequence and 3D information from atomic structures of proteins. Nucleic Acids Res 2003;31: 3320–3.
[42] Krissinel E, Henrick K. Inference of macromolecular assemblies from crystalline state. J Mol Biol 2007;372:774–97.
[43] Glaser F, Pupko T, Paz I, Bell RE, Bechor-Shental D, Martz E, et al. ConSurf: identification of functional regions in proteins by surface-mapping of phylogenetic information. Bioinformatics 2003;19:163–4.
[44] Landau M, Mayrose I, Rosenberg Y, Glaser F, Martz E, Pupko T, et al. ConSurf 2005: the projection of evolutionary conservation scores of residues on protein structures. Nucleic Acids Res 2005;33:W299–302.